Fast aggregation of colloidal silica

James E. Martin, Jess P. Wilcoxon, Dale Schaefer, and Judy Odinek
Sandia National Laboratories, Albuquerque, New Mexico 87185
(Received 6 November 1989)

The aggregation kinetics of colloidal silica is highly dependent on conditions such as the *p*H and salt concentration. In this paper we investigate the aggregation of colloidal silica under conditions that promote rapid growth, contrasting our findings with earlier investigations of the slow growth of silica. A number of interesting effects are observed, including power-law growth of the mean aggregate radius, dependence of the aggregation rate on concentration and the chemical nature of the salt used, a reduced aggregate fractal dimension, fragmentation of the fast aggregates under changing solution conditions, and shear-induced restructuring of aggregates. Finally, we present evidence that the fractal dimension of aggregates is not strongly universal, but depends weakly on such factors as the solution concentration. We conclude that although the diffusion-limited cluster-cluster aggregation model gives a good first-order description of rapid aggregation, real systems exhibit richer behavior that is not given to such a facile interpretation.

I. INTRODUCTION

The chemistry of silica is very rich, involving aspects of colloid formation, aggregation under reaction- or diffusion-limited conditions, and chemical gelation. Indeed, during the formation of a silica gel from a monomer such as tetramethoxysilicon the system can evolve through each of these regimes of growth.[1] At this time, detailed studies of the critical growth that occurs near the gel point have been reported,[2,3] and the aggregation of colloidal silica has been extensively studied under reaction-limited conditions,[4–6] where exponential growth of clusters of fractal dimension $D=2.05\pm0.06$ is observed. However, relatively little work[6,7] has been done on the aggregation of silica under conditions that promote rapid aggregation. In this paper we present an investigation of colloidal silica aggregation under rapid growth conditions, contrasting these findings with slow aggregation of silica.

Elastic and quasielastic light scattering are employed to resolve a number of issues concerning silica aggregation: the determination of the fractal dimension under a variety of growth conditions; the concentration, *p*H, salt, and temperature dependence of the growth kinetics; scaling of the cluster size distribution; fragmentation processes that accompany changing solution conditions or shear; and restructuring of the aggregates. In contrast to the behavior of slow aggregates, we find a smaller fractal dimension of $D=1.73\pm0.06$; growth that is in accord with the diffusion-limited prediction of the cluster mass growing linearly with time; a complex concentration, *p*H, and temperature dependence of growth; sensitivity of the aggregates to shear and changing solution conditions (slow aggregates are very robust); and specific counter-ion effects that violate the simple screened Coulomb potential picture of colloidal interactions. These effects underline the complexity of hydrophilic colloid behavior.

II. KINETICS OF GROWTH

A. The kinetic rate equation

At the simplest level there are two fundamental issues of aggregate formation—the kinetics of growth and the relation of this to the resulting fractal structure of the aggregates. Although investigations of aggregate structure depend on simulations of growth, the Smoluchowski[8] or kinetic rate equation provides a useful analytic mean-field approach to the kinetics, and provides a framework in which to classify a variety of growth processes. This classification helps to clarify the difference between aggregation and gelation processes, both of which we observe in silica.

The Smoluchowski equation expresses the time evolution of the number of m-mers, $N(m)$, in terms of a reaction kernel K_{ij}, which gives the probability of an i-mer reacting with a j-mer.

$$\frac{dN(m)}{dt}=\frac{1}{2}\sum_{\substack{i,j\\ i+j=m}} N(i)K_{ij}N(j)-N(m)\sum_{j} K_{mj}N(j)\ . \tag{1}$$

The first term accounts for the creation of m-mers through binary collisions of i-mers and $(m\text{-}i)$-mers; the second term represents the "annihilation" of m-mers due to binary collisions with other clusters. Although the structure of this equation is simple, it is difficult to determine the form of the reaction kernel for a given physical system.

Van Dongen and Ernst[9] have introduced a classification scheme for *homogeneous* kernels, based on the relative probabilities of large clusters sticking to large clusters, and small clusters sticking to large clusters. Depending on which of these processes dominates, one ob-

tains quite different growth kinetics and size distributions. If small-large interactions dominate, then large variations in cluster mass are discouraged, and the size distributions will tend to be tightly bunched, like a bell-shaped curve. On the other hand, if large-large interactions dominate, then the small clusters tend to get left behind in the scramble and a monotonically decreasing size distribution (with a power-law decay) is obtained. To clarify our studies of growth we give a brief summary of the pertinent results.

The growth classes can be defined by two exponents. Let the probability that a j-mer reacts with a j-mer (large with large) be $K_{jj} \sim j^{\lambda}$, and let the probability that a j-mer reacts with a monomer (large with small) be $K_{1j} \sim j^{\nu}$. Based on these exponents, a few general comments can be made about homogeneous kernels. First, kernels with either $\lambda > 2$ or $\nu > 1$ are unphysical, since the reactivity cannot increase more rapidly than the cluster mass j. Second, if λ is greater than 1 the Smoluchowski equation predicts the formation of an infinite cluster in finite time—a gel point. Finally, kernels with $\lambda \leq 1$ give nongelling behavior, that is, an infinite cluster is formed at infinite time, so much of the qualitative behavior of the Smoluchowski equation is controlled by λ.

In class I growth large-large interactions dominate, i.e., $\lambda > \nu$; this class is relevant to gelation, and may be relevant to aggregation as well. In the nongelling regime, where $\lambda < 1$, the number distribution decays algebraically like $N(m) \sim m^{-\tau}$, with $\tau = 1 + \lambda$, and the weight-average mass M_w grows as a power of time $M_w \sim t^z$ with $z = 1/(1-\lambda)$. We note that since $\lambda < 1$, the *polydispersity exponent* τ is less than 2, in contrast to systems which exhibit a gel point, where τ is greater than 2. Also, as λ approaches 1 the growth exponent $z \to \infty$ —in this limit the growth becomes exponential in time.

The gelling regime of class I growth, where $\nu < 1 < \lambda \leq 2$, the number distribution again exhibits a power-law decay $N(m) \sim m^{-\tau}$ with $\tau = (\lambda + 3)/2 > 2$. Below the gel point this algebraic decay is valid only for clusters smaller than the typical cluster size $M_z = \sum_m m^3 N(m) / \sum_m m^2 N(m)$. However, above t_{gel} this algebraic decay extends to arbitrarily large clusters, and the prefactor of the decay decreases monotonically with time, as clusters bond to the infinite cluster. Near the gel point M_w diverges like $|t_{\text{gel}} - t|^{-\gamma}$, where $\gamma = 1/(\lambda - 1)$, and the mean cluster size M_z diverges like $|t_{\text{gel}} - t|^{-1/\sigma}$, where $\sigma = (\lambda - 1)/2$. Thus for homogeneous gelling kernels the Smoluchowski equation predicts $M_w \sim M_z^{1/2}$.

Class III growth, defined by the domination of small-large interactions, appears to be a good description of aggregation under diffusion-limited conditions. However, since ν must always be less than 1 and by definition λ must be less than ν, a gel point is not possible in this class of growth. Because small-large interactions give negative feedback, large polydispersity is discouraged, and size distributions tend to be tightly bunched, as in a bell-shaped curve.

The original Smoluchowski kernel,[8] developed to describe *diffusion-limited* aggregation, gives the reaction rate as a collision cross section due to diffusion of spheres

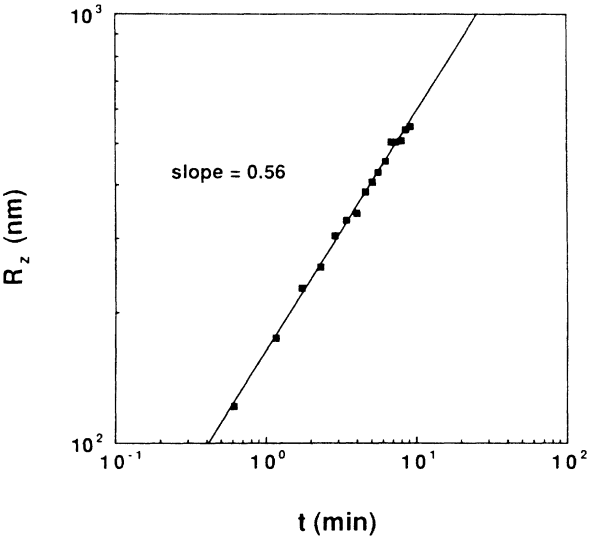

FIG. 1. Quasielastic light-scattering measurements of the rapid aggregation of colloidal silica give power-law growth of the cluster radius with time, in this case with $R \sim t^{0.56}$. These data were taken by aggregating a concentration of 4.0×10^{-2} wt. % 11-nm radius colloidal silica at pH 8.5. Clusters 1 μm in size are produced in about 24 min.

of radius R, having the diffusion constant $D = kT/6\pi\eta R$. The result $K_{ij} = (R_i + R_j)(D_i + D_j) \propto (i^{1/3} + j^{1/3})(i^{-1/3} + j^{-1/3})$ is a class III kernel with $\nu = \frac{1}{3}$ and $\lambda = 0$. Of course, recent experiments show that aggregates are fractal objects of dimension D, so the exponent $\frac{1}{3}$ should be modified to $1/D$ —a minor point.

Class II growth is a complex intermediate between class I and class III growth. In class II growth $\lambda = \nu \leq 1$, so neither small-large nor large-large interactions are dominant. Again, since $\lambda \leq 1$ no gel point is possible. Sum kernels of the form $(i^a + j^a)^b$ are examples of class II kernels. Although little is known about the size distributions for class II kernels, for $\lambda = 1$ the growth of the average mass is known to be exponential in time, which suggests that class II kernels are relevant to aggregation under *reaction-limited* conditions.

In summary, the kinetic rate equation predicts three qualitatively distinct behaviors of growth.

Power-law growth:

$$M_w \sim t^z, \quad z = 1/(1-\lambda) .$$

Exponential growth:

$$M_w \sim e^{ct} .$$

Gel growth:

$$M_w \sim |t_{\text{gel}} - t|^{-\gamma}, \quad \gamma = 1/(\lambda - 1) .$$

In silica systems, experimental evidence exists for all three types of growth. For example, when an orthosilicate is reacted under alkaline conditions, small colloidal particles are formed. The colloidal suspension can then be destabilized by either adding salt and or adjusting the pH, so that the colloidal particles aggregate. If the ag-

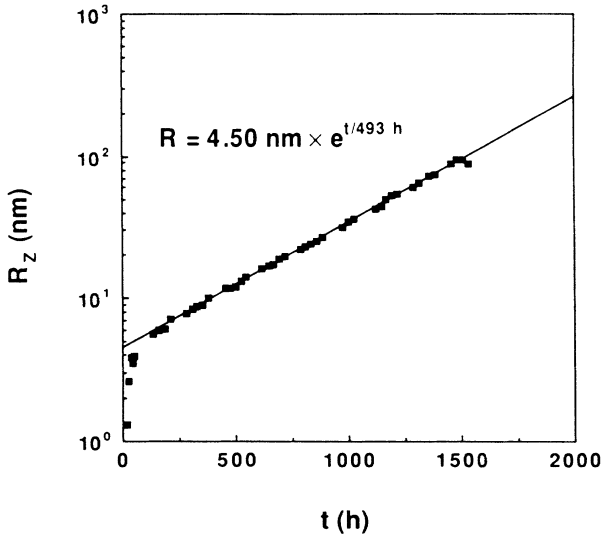

FIG. 2. Exponential growth of the mean cluster size is observed under slow reaction conditions. In this case 4.5-nm radius colloidal particles were grown by catalyzing hydrolysis and condensation of 0.06M tetramethoxysilicon at high pH. The rapidly formed, highly charged colloids then react extremely slowly to form aggregates with fractal dimension 2.05±0.06. In this sample clusters reach a radius of 100 nm after ~1500 h. In a rapidly aggregating system at comparable concentration, 100-nm aggregates would be produced in a few seconds.

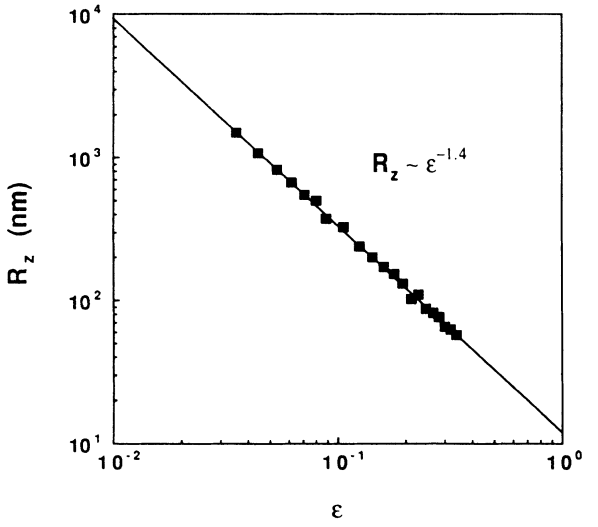

FIG. 3. Critical growth of silica is observed in the vicinity of the gel time t_{gel} [$\epsilon=(t_{gel}-t)/t_{gel}$]. In this case a gel was produced by a sequential acid-base catalysis of 1.0M tetramethoxysilicon in methanol with 4.0M H_2O. At very early times colloidal particles are formed. These then aggregate until the volume fraction of aggregates is 1, at which point the connectivity divergence is observed (measurements were made on diluted clusters).

gregation process proceeds rapidly, power-law growth is observed,[7] as shown in Fig. 1. On the other hand, if the aggregation process proceeds slowly, exponential growth of the average cluster mass is observed,[1-4] as in Fig. 2. Under appropriate reaction conditions, colloidal particles are formed that undergo reaction-limited aggregation and finally form gels. In the vicinity of the gel point the system undergoes a crossover from aggregation to gelation,[1] and exhibits the power-law divergence[3] shown in Fig. 3. Having given this brief overview of growth processes in silica we will now focus our attention on the rapid aggregation regime.

B. Cluster radius from quasielastic light scattering

Studies of growth of colloidal silica require some method to determine the cluster radius. Static light scattering would permit such studies under restricted length scale regime, but quasielastic light scattering allows, in principle, radius measurements over several orders of magnitude. How many orders of magnitude are possible is extremely dependent on the class of growth that is being studied, and so this technique is very often misapplied. In the following, we will discuss the application of this technique to the study of growth processes, with particular emphasis on rapid aggregation.

From quasielastic light scattering (QELS) one can obtain information about the size of an object by determining the relaxation time associated with translational, rotational, or "configurational" diffusion. In the case of a monodisperse solution of spheres the size information thus obtained is unambiguous, but in general effects of polydispersity and internal modes can seriously compromise the interpretation of the data. In a quasielastic light-scattering experiment, the intensity $I(q)$ of light scattered at wave vector q is autocorrelated to obtain the homodyne correlation function[10] $C(t)=\langle I(q,0)I(q,t)\rangle$. The dynamic structure factor $S(q,t)$ is then obtained from the standard relation

$$S(q,t)=[C(t)-\langle I(q,0)I(q,\infty)\rangle]^{1/2} .$$

In the simple case of monodisperse spheres the dynamic structure factor is given by $S(q,t)=S(q)\exp(-q^2D_t t)$, where $S(q)$ is the static structure factor, $D_t=kT/6\pi\eta R$ is the translational diffusion coefficient, and R is the hydrodynamic radius. The physical interpretation is clear enough; the relaxation time $1/(q^2D_t)$ is just the time it takes a sphere to diffuse a distance $1/q$. For nonspherical rigid objects, such as a rigid rod, rotational motions can contribute to the scattering in the regime $qR \gg 1$, where R is the rod length. Likewise, for flexible objects such as linear polymers configurational relaxations can contribute to the dynamic structure factor when $qR \gg 1$. However, in the absence of depolarized scattering, a condition that is met for simple dielectric aggregates such as silica, only translational diffusion contributes to the scattering when $qR \ll 1$. Thus in this regime the dynamic structure factor may be written $S(q,t)=S(q)\exp(-q^2D_t t)$ where $S(q)$ is the structure factor for an aggregate. The initial decay rate, or first cumulant $\Gamma=-d\ln S(q,t\to 0)/dt$, is

then just q^2D_t.

Of course, measurements are virtually never taken on monodisperse systems so it is important to consider the effect polydispersity can have on the dynamics,[11,12] even in the absence of further complications due to internal modes. The polydispersity averaged correlation function is just

$$S(q,t)=\int_0^\infty m^2N(m)S_m(q,t)dm \tag{2}$$

so the average first cumulant is

$$\Gamma/q^2=\int_0^\infty D_t(m)m^2N(m) \times S_m(q)dm \Big/ \int_0^\infty m^2N(m)S_m(q)dm \ . \tag{3}$$

This expression warrants some discussion. First, in the regime where $qR_z \ll 1$ we obtain the relation $\Gamma/q^2=D_z$, where the subscript z denotes the so-called z average, which is the average of any quantity over $m^2N(m)$. [Note that although the z-average radius observed in an elastic light-scattering experiment is the root-mean-square average $(\langle R^2\rangle_z)^{1/2}$, the z average observed in a quasielastic light scattering experiment is the harmonic average $\langle R^{-1}\rangle_z^{-1}$.] Only in this limit can R_z be extracted from the relation $D_z=kT/6\pi\eta R_z$. In a quasielastic light scattering experiment with a He-Ne laser operating at 633 nm and at a typical scattering angle of 90°, $1/q=54$ nm for aqueous samples. When the aggregate size exceeds 54 nm the interpretation of the data becomes more complex. However, with reasonable care, measurements can be routinely run at a scattering angle of 10° or $1/q=438$ nm, which significantly extends the resolution of the technique. Early quasielastic light-scattering measurements of colloidal silica aggregates[13] were made at angles as low as 3.8°, corresponding to the length scale $1/q=1150$ nm.

However, we are interested in understanding what happens when we greatly exceed the instrumental resolution, so that $qR_z \gg 1$. The behavior of Eq. (3) in this regime depends greatly on the polydispersity. For the purpose of this discussion it is useful to define an apparent hydrodynamic radius $R_{\rm app}$ through the relation $\Gamma/q^2=kT/6\pi\eta R_{\rm app}$. We find that the behavior of $R_{\rm app}$ at large qR_z depends very much on the value of τ in the relation $N(m)=m^{-\tau}$ and therefore on the class of growth we are investigating. In the regime $qR_z \gg 1$ the general result is

$$R_{\rm app}=\frac{R_z}{(qR_z)^\alpha} \tag{4}$$

where α is an exponent that depends on D and τ. There are three regimes of polydispersity,[12] which we refer to as weak, intermediate, and strong:

$$\alpha=\begin{cases} 0, & \tau<2-1/D \ \text{(weak)} \\ 1-D(2-\tau), & 2-1/D<\tau<2 \ \text{(intermediate)} \\ 1, & \tau>2 \ \text{(strong)}. \end{cases}$$

The strong regime, where $\tau>2$, corresponds to a system which has a sol-gel transition, and therefore is valid when critical growth is observed. In this case the apparent radius $R_{\rm app}\sim 1/q$ contains absolutely no information about the actual size of the clusters being formed and so measurements must be taken in the regime $qR_z \ll 1$. This *length-scale-independent* behavior of the apparent radius is demonstrated for gelling silica[3] in Fig. 4.

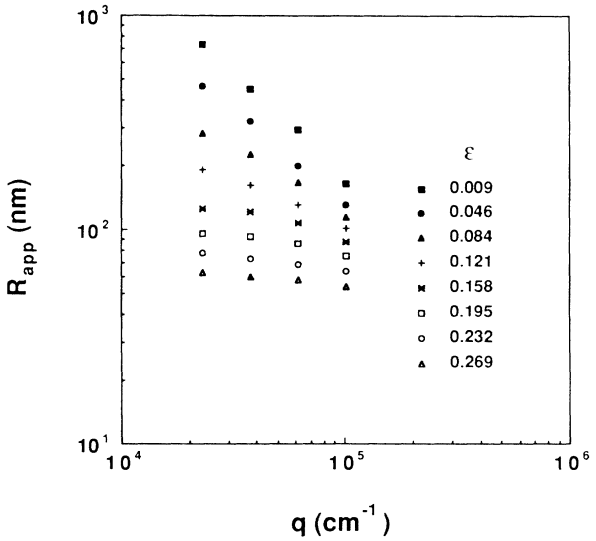

FIG. 4. In a system that exhibits critical growth (i.e., $R\sim\Delta t^{-\nu}$) the apparent radius taken from quasielastic light scattering becomes *length-scale independent* in the regime where $qR_z \gg 1$. Thus a slow progression is observed from $R_{\rm app}=R_z$ for samples at early times to $R_{\rm app}\sim q^{-1}$ near the gel point (small ϵ). Since in this regime $R_{\rm app}$ carries no information about the mean clusters size R_z, the resolution of QELS is seriously compromised in critical studies of any type. These data were taken from a 1.0M silica gel.

The intermediate regime, where $R_{\rm app}\sim R_z^{D(2-\tau)}/q^{1-D(2-\tau)}$, is relevant to slow aggregation where exponential growth is observed. Measurements on slow aggregates[4,13] (Fig. 5), demonstrate that $R_{\rm app}\sim R_z^{0.3}/q^{-.7}$, indicating a polydispersity exponent $\tau=1.85$. Since the true cluster radius appears in this expression it is possible to obtain size information in this large qR_z regime.

Fortunately, power-law growth of silica falls in the weak-polydispersity regime, where $R_{\rm app}=R_z$. An example of this is shown in Fig. 6, where the q dependence of $R_{\rm app}$ is shown for fast aggregates of colloidal silica. To a fair degree it is observed that the apparent radius is q independent, even though the measurements were made at very high values of qR_z. In fact, since the polydispersity does not introduce any power-law dependence of $R_{\rm app}$ on q, more subtle effects can be observed. For example, at large q the structure factor of an aggregate is $S(q)\sim(qR)^{-D}$; if this is substituted into Eq. (3) it is observed that the weight-average diffusion coefficient D_w [average of D_t over $mN(m)$] is observed at large qR_z. Thus in the limit of large qR_z we obtain $R_{\rm app}=R_w$ where $R_w=kT/6\pi\eta D_w$. The magnitude of this effect is easily computed: using the universal exponential cutoff for the exponential tail of the size distribution we obtain

$$\frac{R_z}{R_w}=\frac{2-\tau}{2-1/D-\tau} \ . \tag{5}$$

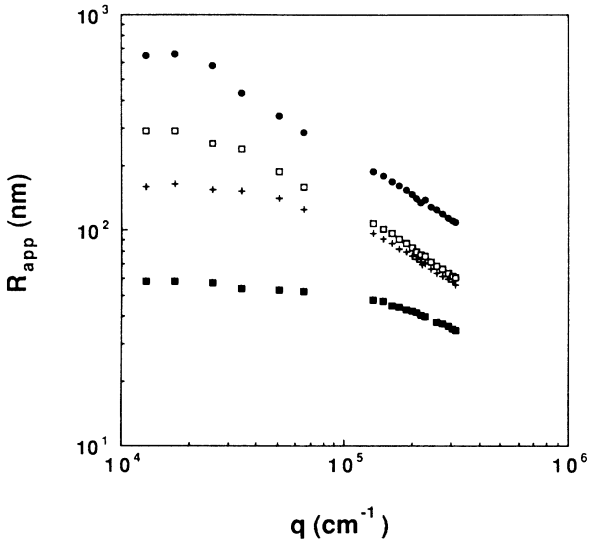

FIG. 5. Quasielastic light scattering measurements on colloidal silica aggregates grown under slow conditions (*p*H 5.5, 0.07*M* NaCl, 60°C) give $R_{app} \sim R_z^{0.35}/q^{0.65}$ in the regime $qR_z > 1$. From bottom to top, these curves were taken from 40, 60, 80, and 100 h of growth. Thus the mean cluster radius can be extracted from the data, but only after properly accounting for the q dependence of the apparent radius.

In the constant kernel approximation, the Smoluchowski equation predicts $\tau=0$ so $R_z/R_w=\frac{4}{3}$, a rather minor effect. Rotational effects can also be observed when the polydispersity is very weak, but the effect is small, being comparable to the weak polydispersity effect itself. Note that Eq. (5) diverges when $\tau=2-1/D$, which marks the crossover from weak to intermediate polydispersity. This is because we have already taken the large wave-vector limit $q=\infty$ in obtaining Eq. (5).

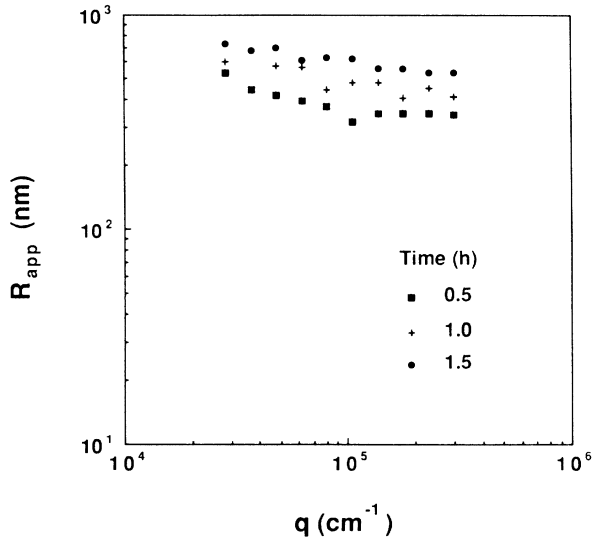

FIG. 6. Very rapid quasielastic light scattering measurements from a 2.5×10^{-4}% solution of colloidal silica at *p*H 8.5 give only a weak q dependence of the apparent radius in the regime $qR_z \gg 1$. This relatively small q dependence is a result of the weak polydispersity and the small degree of form isotropy in the system. In fact, simulations (Ref. 14) show that the principal axes of the inertial tensor for fast aggregates are nearly equal.

In summary, then, we have shown that (i) polydispersity severely limits the instrumental resolution in studies of critical growth where $\tau>2$; (ii) quasielastic light-scattering studies of exponential growth can still yield size information when $qR_z \gg 1$, but care must be used to extract the true radius from the apparent, wave-vector-dependent radius; and (iii) in power-law growth the effect of polydispersity is essentially benign, allowing useful size information to be obtained even in the limit as $qR_z \gg 1$.

Another issue arises in studies of fast aggregation. Because of the rapid rates of growth that are frequently observed, aggregates can grow appreciably during the signal averaging required to obtain a low-noise autocorrelation function. The hydrodynamic radius obtained from the first cumulant of the intensity autocorrelation function is thus larger than the true radius at the beginning of the run, but smaller than the true radius at the end of the run. At some time during the run the true radius is the same as the measured radius, and this is the time we must use in the analysis of our data.

The general expression for the time-averaged first cumulant is

$$\Gamma=\frac{\int_{t_i}^{t_f}\Gamma(t)S_w(t)dt}{\int_{t_i}^{t_f}S_w(t)dt} \tag{6}$$

where $\Gamma(t)$ is the true first cumulant at time t, t_i and t_f are the initial and final time of the run, and $S_w(t)=\sum_m m^2N(m)S_m(q)$ is the weight-average static structure factor at time t. It is useful to consider the behavior of Eq. (6) in two limits; $qR_z \gg 1$ and $qR_z \ll 1$. We consider the large-wave-vector intermediate scattering limit first.

In the large-wave-vector regime the static scattering from the fractal aggregates becomes independent of the mean radius, and therefore of time, so $S_w(t)$ is a constant. Equation (6) then reduces to

$$\Gamma=\frac{1}{\Delta t}\int_{t_i}^{t_f}\Gamma(t)dt\ , \tag{7}$$

where $\Delta t=t_f-t_i$. In the special case of power-law growth, where the average radius increases as $R_z \sim t^{z/D}$, the result is simple: Define the apparent time t_{app} as the time at which the true mean radius of the system is the same as the measured radius. From Eq. (7) we obtain $t_{app}=t_i+\Delta t/2[1+O(\Delta t/t_i)]$, so that the apparent time is simply the midpoint of the run time, with a small correction.

In the small-wave-vector regime $S_w(t)$ is just the weight-average cluster mass $M_w \sim t_z$. Substituting this into Eq. (6) gives the same result for the apparent time as the large-wave-vector limit, so as a general rule the midpoint of the run time is the appropriate variable against which to plot mean radius data obtained from quasielastic light scattering. We have consistently used the midpoint in analyzing all of our data.

C. Measurements of cluster growth

The aggregation rate of colloidal silica can be controlled by using salt to screen the surface charge and adjusting the pH to vary the surface charge. The isoelectric point of colloidal silica is $\sim p$H 2.8, and since our studies were done at high pH a substantial negative surface charge was present. Rapid aggregation samples at pH 9.6 were buffered with borax-NaOH solution with 1M NaCl. Samples at pH 8.5 were buffered with borax-HCl solution with 1M NaCl. Finally, pH 6.7 samples were buffered with potassium dihydrogen phosphate–NaOH solution with 1M NaCl. Aggregates were formed at concentrations varying from 1.0×10^{-2} to 2.5×10^{-4} wt. % SiO_2, and the initial colloid radius was $r=11$ nm.

Aggregation studies at pH 8.5 are shown in Fig. 7 and are tabulated in Table I. At all concentrations the growth is well described by a power law, with $R_z\sim t^{0.55\pm0.06}$ over the range of concentrations investigated. Since aggregation is rapid at this pH, it is reasonable to expect growth to be described by the diffusion-limited expression for the reaction kernel $K_{ij}=(R_i+R_j)(D_i+D_j)$. Using the Stokes-Einstein expression $D_i=kT/6\pi\eta R_i$ gives $K_{ij}\sim kT/6\pi\eta$ in the approximation that most collisions occur between clusters of comparable size. This constant kernel predicts a power-law increase in the cluster size with time, $M_w\sim[(kT/6\pi\eta)N_0t]^z$, with the growth exponent $z=1$, or in terms of the mean cluster radius $R_z\sim[(kT/6\pi\eta)N_0t]^{z/D}$. Here N_0 is the initial number density of colloidal particles. Using the observed fractal dimension $D=1.73\pm0.07$ (see below) and the measured values of z/D we conclude that the bulk of the data are described by $z=0.95\pm0.1$, in good agreement with the diffusion-limited prediction $z=1$.

A more sensitive test of diffusion-limited growth is shown in Fig. 8, where the mean number of particles per aggregate $(R/r)^D$ is plotted against $(kT/6\pi\eta)N_0t$ (as a matter of interest, at $c=2.5\times10^{-4}$ wt. % the initial number density N_0 is 2×10^{11} cm^{-3} or 3×10^{-10} M). On these universal axes the data collapse is only marginal, even though the kinetics of growth is apparently diffusion limited at all concentrations. In particular, it is observed that samples at higher concentrations grow more slowly than one might expect, given their initial concentration. This implies a sticking probability (probability that a collision results in sticking) that decreases with increasing concentration.

Rapid aggregation can also be induced at pH 9.6, as shown in Fig. 9. These data have an apparently smaller growth exponent than the pH 8.5 data, with

TABLE I. Fractal dimensions of colloidal silica aggregates.

c (wt. % SiO_2)	pH	D	Salt
0.00025	8.5	1.73	NaCl
0.001	8.5	1.85	NaCl
0.008	8.5	1.89	NaCl
0.01	8.5	1.97	NaCl
0.01	8.5	1.84	CsCl
0.00025	9.6	1.60	NaCl
0.001	9.6	1.75	NaCl
0.01	9.6	1.78	NaCl
0.01	9.6	1.94	CsCl
0.01	9.7	1.98	CsCl rapid
0.01	10	2.30	CsCl slow
0.01	10	1.84	NaCl

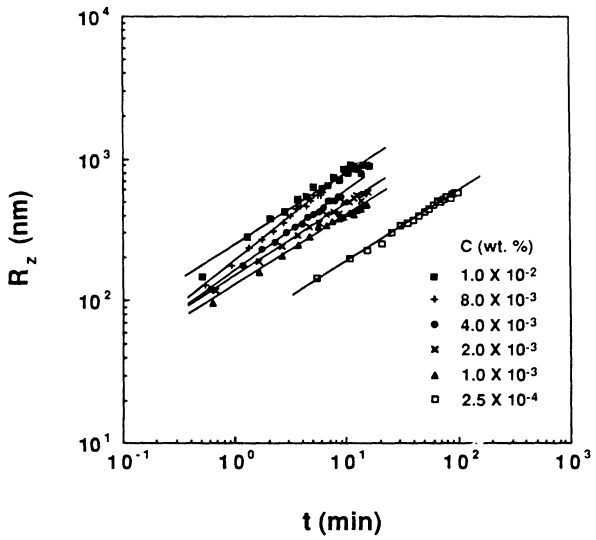

FIG. 7. Power-law growth data for colloidal silica at pH 8.5 is shown as a function of silica concentration. At this pH growth is described by $R_z\sim t^{0.55\pm0.06}$ over the range of concentrations investigated.

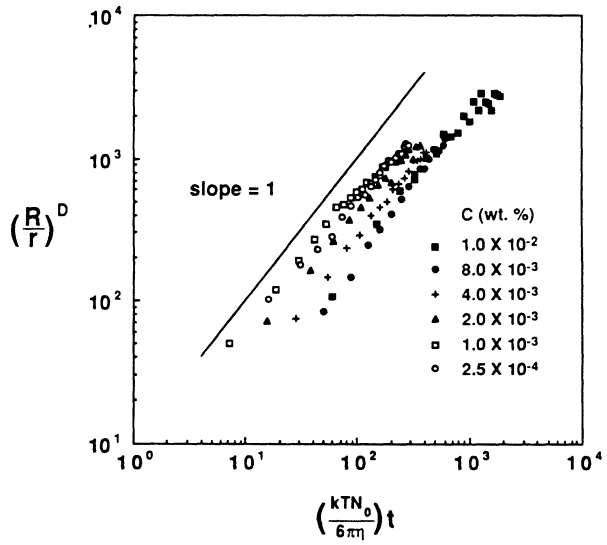

FIG. 8. The growth data in Fig. 7 are plotted to test the Smoluchowski prediction for diffusion-limited growth. Here r is the colloidal radius, N_0 is the initial particle number density, and η is the solvent viscosity. On these axes growth data at all temperatures and concentrations should fall on a master curve with a slope of 1. Although linear growth of the mean cluster mass is observed at any single concentration, growth is slower than expected at the higher concentrations.

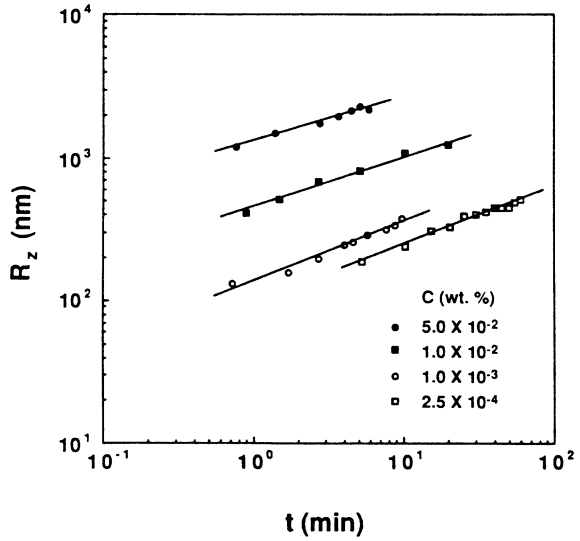

FIG. 9. Power-law growth data taken at pH 9.6 give a somewhat smaller value of the growth exponent than data taken at pH 8.5, with $R \sim t^{0.40\pm0.06}$ describing the data over the range of concentrations investigated.

$z/D = 0.43\pm0.07$ or $z = 0.74\pm0.12$. As we shall discuss, these aggregates are very fragile so it is possible that the lower exponent is due to a competition between aggregation and fragmentation. However, the data collapse in Fig. 10 is substantially better, indicating a less concentration-dependent sticking probability.

Since the mean cluster size scales as $R_z \sim [(kT/6\pi\eta)N_0 t]^{z/D}$ it should be possible to determine z/D by measuring the concentration dependence of R_z at fixed time. Of course, the universal plot in Fig. 8 indicates that this value of z/D will be smaller than the value obtained from the time dependence. The mean radius at 10 min is shown as a function of concentration in Fig. 11 for samples at pH 8.5 and 9.6. The pH data are

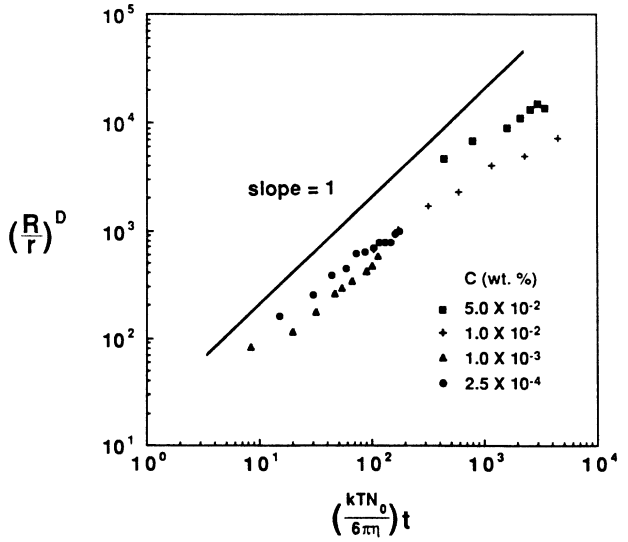

FIG. 10. A better data collapse is observed for aggregates grown at pH 9.6, but the agreement with the Smoluchowski slope of 1 is much worse, perhaps indicating the increasing importance of fragmentation in larger clusters.

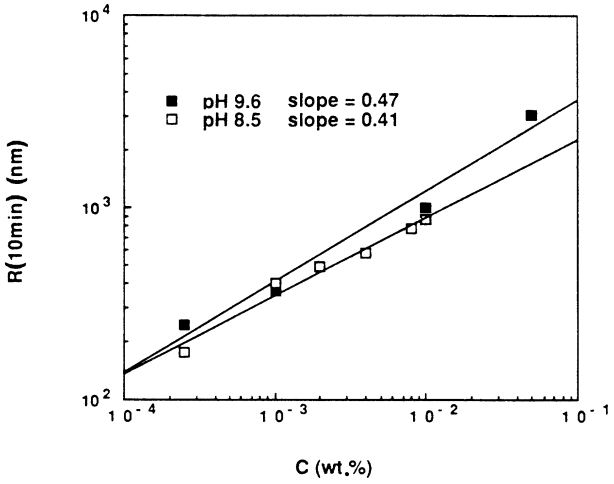

FIG. 11. The mean cluster radius after 10 min of growth is plotted against concentration for samples grown at pH 8.5 and 9.6. The pH 8.5 samples give $R_z \sim c^{0.41\pm0.04}$, whereas the pH 9.6 samples give $R_z \sim c^{0.47\pm0.04}$. These exponents are significantly smaller than the diffusion-limited prediction of $R \sim c^{0.56}$.

best described by $R_z \sim c^{0.47\pm0.05}$ and the pH 8.5 data are described by $R_z \sim c^{0.41\pm0.05}$. Thus the concentration dependence of the pH 8.5 data is anomalously weak. This effect has also been observed in studies of gold aggregation,[15] where $R_z \sim c^{0.38\pm0.05}$.

The anomalous concentration dependence is better illustrated in the following way. If we merely assume that the reaction kernel itself is independent of concentration, then R_z should be a function of $N_0 t$. Thus $1/\tau$, the rate that a cluster reaches 1 μm in radius, should be proportional to the initial concentration, regardless of the form of the kernel. In Fig. 12 this is shown for the data at pH 9.6, where $1/\tau \sim c^{1.09\pm0.15}$, and for pH 8.5, where $1/\tau \sim c^{0.78\pm0.1}$. Thus we observe that close inspection of the pH 8.5 data reveals that the data cannot be simply

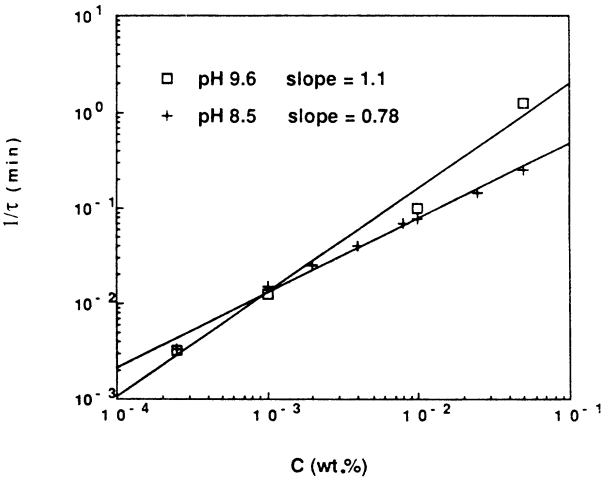

FIG. 12. The inverse growth time to 1 μm is plotted vs concentration for aggregation at pH 8.5 and 9.6. If the kernel in the Smoluchowski equation is concentration independent then $1/\tau \sim c^1$. Although the pH 9.6 data agree with this prediction, the pH 8.5 data give $1/\tau \sim c^{0.78}$, indicating slower than expected growth at higher concentrations.

described in terms of the diffusion-limited growth model.

In conclusion, the growth we have observed is in reasonably good agreement with the predictions of the Smoluchowski equation with the diffusion-limited kernel, when only the time dependence of the growth is considered. The somewhat smaller value of z observed in the pH 9.6 case may be a result of competing fragmentation processes that become dominant at large cluster sizes. However, larger discrepancies are observed when the concentration dependence of the growth is analyzed. At pH 8.5, growth is slower than expected based on the diffusion-limited approximation or the fundamental form of the Smoluchowski equation. This may be due to a reduced sticking probability at higher concentrations, which may in turn be due to the presence of a surface active stabilizing agent in the original colloidal silica. It is known that a system with a small but finite sticking probability ultimately crosses over from reaction- to diffusion-limited growth. Thus with a concentration-dependent sticking probability it is possible to observe diffusion-limited behavior in the time domain without observing diffusion-limited growth in the concentration domain.

III. STRUCTURE OF AGGREGATES

A. Fractal models of aggregation

Having ascertained that the growth kinetics is in reasonable agreement with the diffusion-limited model, it is of interest to measure the structure of these colloidal aggregates. There is considerable controversy surrounding this issue as a result of the disparate plenitudinous results reported thus far for a variety of systems. In fact, much of the recent interest in aggregation has centered on the observation that the scattering behavior of these systems indicates a mass fractal structure (in a mass fractal the radius R increases with mass M as $M \sim R^D$, where D is the fractal dimension). In retrospect, this fractal structure seems natural since the growth of aggregates is hierarchical in nature: small clusters collide to form large clusters, which collide to form larger clusters *ad infinitum*. As long as the relative interpenetration that occurs in these collisions is independent of scale, self-similarity is certain. In this section we explore the dependence of the aggregate fractal dimension on colloid concentration, solution pH, and specific salt.

One of the earliest models of aggregation[14] is the so-called diffusion-limited aggregation model (DLA), in which aggregation is envisioned by the irreversible sticking of Brownian monomers to a seed cluster. This *particle-cluster* model captures the striking self-similarity of aggregates, but predicts a rather large fractal dimension of $D = 2.5$. It became immediately apparent that a physically tenable model of aggregation must include collisions between all possible species, monomers and clusters. At this time it is thought that there are two limiting regimes of cluster-cluster growth: the diffusion limited regime, where clusters have a sticking probability of unity, and the reaction-limited regime, where particles have a sticking probability approach zero. Simulations of the diffusion-limited model, with power-law growth, give a fractal dimension of $D = 1.75$ [Fig. 13(a)] and reaction-limited simulations give more compact clusters, with $D = 2.05$ [Fig. 13(b)]. Exponential growth is observed experimentally in the latter regime. This is a major discrepancy between experiment and simulation and serves to discombobulate the current theoretical understanding of aggregation.

Whenever scaling behavior is found it is tempting to believe that some kind of universality underlies the observed behavior. Hopefully, the experimental system then falls into a few relatively simple universality classes. Results that don't fit into established modes of scaling behavior are often assumed to be in a crossover regime of one sort or another. However, some features of aggregation, such as the ability of the clusters to rearrange, are too complex to simulate, yet may be important in real systems. Thus these limiting regimes must be thought of as the simplest behavior aggregating systems can exhibit,

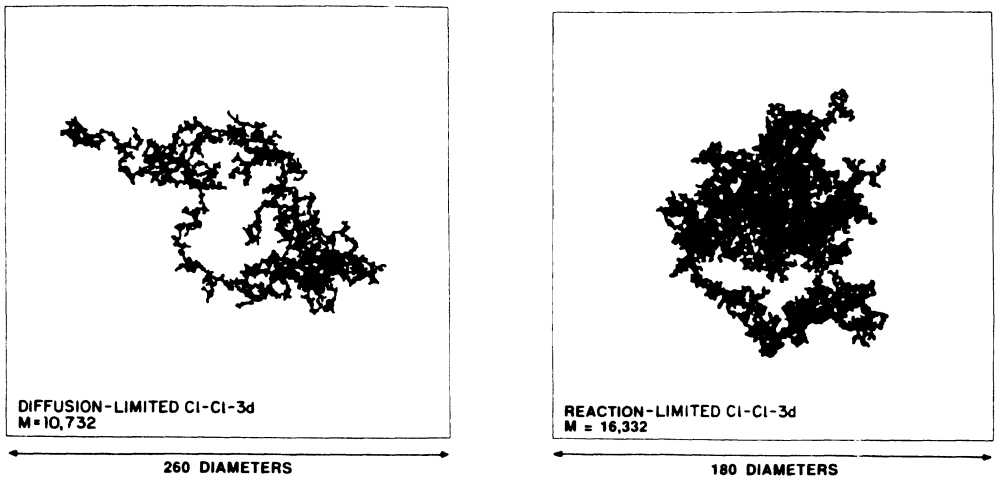

FIG. 13. A 3-d diffusion-limited cluster-cluster aggregate (a) is compared to a 3-d reaction-limited cluster-cluster aggregate (b). Simulations give a fractal dimension of ~ 1.75 for diffusion-limited aggregates and 2.05 for reaction-limited aggregates. These features are courtesy of P. Meakin.

and do not necessarily manifest the full range of behavior possible in physical systems. In fact, an important issue in aggregation is whether or not the kinetics of growth is a strong determinant in the structure of the aggregates. In the following we will discuss how concentration, growth kinetics, and pH affect the fractal dimension in aggregating systems.

B. Elastic light scattering

Early attempts to measure the fractal dimension of aggregates involved depositing clusters on a substrate and using electron microscopy to obtain an image that could then be analyzed by simple statistical techniques (pair-correlation function or "sandbox" scaling) to obtain the fractal dimension.[16,17] In this approach problems arise due to the difficulty in preventing further high-concentration aggregation of clusters as the sample is deposited on the substrate, and in dealing with the distortion of the aggregates as they are collapsed into two dimensions. Also, such studies must be limited to fractal objects with dimensions less then 2, since objects of greater dimensions cast a solid shadow onto the plane.

Because of the difficulties inherent in the electron microscopy techniques, it was quickly recognized that scattering is the technique of choice for the investigation of fractal structure. In a scattering experiment the intensity I is determined as a function of the length $1/q$. For a *coherent* scattering process, such as light scattering, the interpretation of scattering data from a monodisperse solution is straightforward: *the intensity per unit concentration c is a measure of the average mass in a box of length* $1/q$. Thus for sufficiently small lengths $1/q \ll R$ the fractal relation $M \sim R^D$ becomes $I/c \sim 1/q^D$. Of course, if the length $1/q$ approaches the radius r of the colloidal particles from which the aggregates are grown, fractal scattering behavior crosses over to the classical Porod result for scattering from a sharp interface $I \sim 1/q$.[4] Thus fractal scaling is observed only in the regime $r \ll 1/q \ll R$. In the vicinity of a sol-gel transition the very broad distribution of cluster masses can alter the relation $I/c \sim 1/q^D$ but for the aggregation of silica this relation is valid.

Scattering experiments are usually made with light, neutrons, or x rays. For growth processes such as aggregation, where the clusters can become very large and the fundamental colloid size is already ~ 10 nm, light scattering offers the most accurate method of determining the fractal dimension, for several reasons. First, light scattering can easily explore length scales $1/q$ from 25 to 1000 nm—an ideal match for aggregates. X-ray and neutron-scattering results are usually limited to lengths from 0.1 to 20 nm, and since particle sizes are typically of the order of 10 nm, often only a crossover to fractal scattering behavior can be observed.

Second, incident light fluxes tend to be very high and photon detectors have high quantum efficiency and low dark count. Thus it is easy to run very low sample concentrations, of order 10^{-7} g/ml; by contrast, x-ray and neutron-scattering measurements are often made at 10^{-1} to 10^{-2} g/ml where the effect of interparticle interactions can be important. In fact, at such high concentrations intercluster interactions can dominate the scattering, making a fractal interpretation of the data otiose. Third, light-scattering measurements are made with a "pinhole-collimated" beam, so "desmearing" corrections need not be made to the data, as in x-ray scattering measurements made with a slit-collimated beam (Kratky camera). Desmearing is an ill-conditioned inverse transform problem, so in some of the x-ray scattering data reported for fractal systems no attempt at desmearing the data has been made. It should be mentioned that some investigators have reported impressive scattering data despite these difficulties, but the expertise required is substantial.

C. Measurements of the fractal dimension

Elastic light-scattering measurements were made at silica concentrations ranging from $c = 2.5 \times 10^{-4}$ wt. % to 10^{-2} wt. %. At the highest concentration, growth was rapid, with 1000-nm clusters being produced from 11.0-nm radius colloidal silica in about 0.8 min. Light-scattering data can take several minutes to collect, so measurements are appreciably smeared in time, which might lead to some questions about the validity of these data. In fact, these measurements are valid only because the system is mass fractal. In a mass fractal system the scattered intensity at wave vector q is independent of the

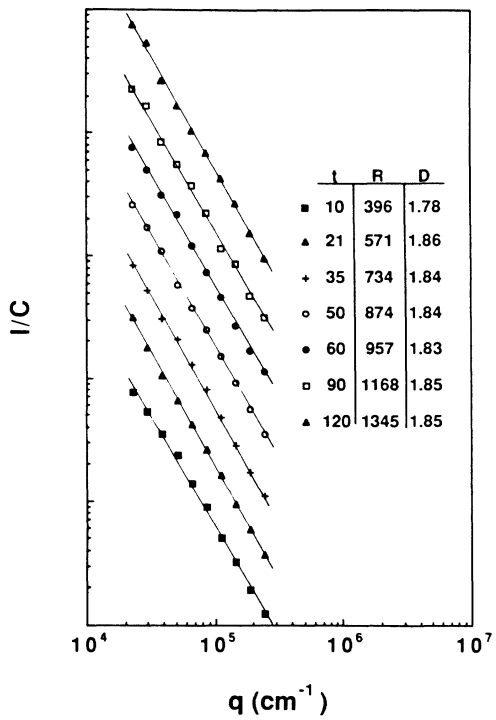

FIG. 14. Time-resolved elastic light-scattering data for rapid aggregates grown at pH 8.5 and a concentration of 10^{-3}% silica show a time-independent fractal scattering, with $I/c \sim q^{-1.84}$, over a large time regime (scattering curves have been vertically shifted for clarity). At the earliest time a slight departure from power-law scattering is observed, due to the proximity of the low-q data to the crossover to the Guinier regime, but spontaneous restructuring was not observed.

cluster radius if $qR \gg 1$ (conservation of mass). Thus the fact that the clusters grow appreciably during the duration of the measurements is unimportant as long as $qR_z \gg 1$. For example, at pH 8.5 and a concentration of 10^{-3} wt. %, 1000-nm clusters are produced in 66 min. Time-resolved scattering data, shown in Fig. 14, demonstrate that the observed scattering, and thus the fractal dimension $D = 1.84$, is independent of time. Thus in our system we do not observe the "restructuring" of silica aggregates that has been observed previously.[6] It is conceivable that this stability is due to the presence of a buffer in our solutions. However, at very large times the scattered intensity actually decreases, due to the sedimentation of large clusters from solution. For example, if a rapidly aggregating sample is allowed to age overnight then the clusters will have formed a delicate, easily resuspended precipitate on the bottom of the scattering cell. Subsequent scattering measurements on the *resuspended* clusters then give a larger fractal dimension, as discussed below.

In Fig. 15 scattering data for rapid aggregates formed at a concentration of 2.5×10^{-4} wt. % silica are contrasted with scattering data for aggregates grown under slow conditions at a concentration of 10^{-1} wt. %. The change in fractal dimension with $D = 1.73 \pm 0.07$ to 2.05 ± 0.06 is apparently in agreement with simulations of diffusion-limited and reaction-limited aggregation,[14] however, the situation is really not so clear. The data in Table II show that the fractal dimension of rapid aggregates increases with concentration, even though the kinetics is always power law. Since slow aggregation is done at high silica concentrations it is unknown if the fractal dimension is concentration dependent. Thus a facile explanation of aggregation in terms of two simple universality classes is yet unproven by extant experimental evidence.

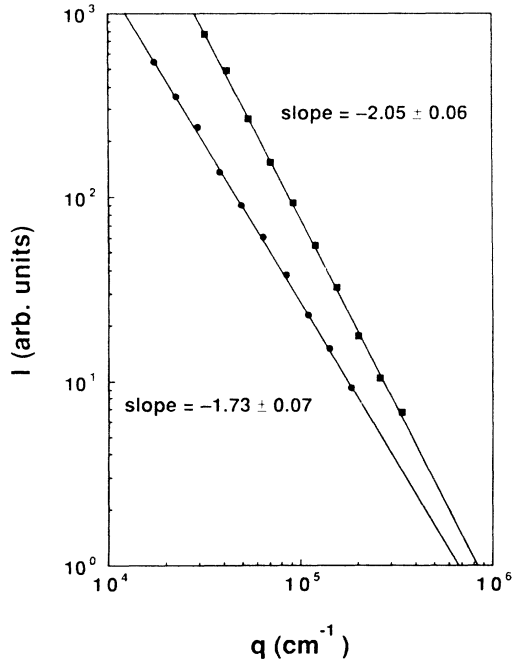

FIG. 15. Light scattering on rapid aggregates at $c = 2.5 \times 10^{-4}$ give a fractal dimension of 1.73 ± 0.07, in contrast with data for slowly grown aggregates, which gives $D = 2.05 \pm 0.06$. These dimensions agree with aggregation simulations (Ref. 14).

TABLE II. Growth exponents for colloidal silica aggregates.

c (wt. % SiO_2)	pH	T (°C)	z/D	z	τ (min)
0.00025	8.5	25	0.52	0.90	297.9
0.001	8.5	25	0.49	0.85	65.7
0.002	8.5	25	0.52	0.90	39.9
0.004	8.5	40	0.57	0.98	16.2
0.004	8.5	25	0.55	0.94	24.6
0.004	8.5	5	0.60	1.04	32.8
0.008	8.5	25	0.62	1.07	14.3
0.01	8.5	25	0.59	1.02	12.7
0.025	8.5	25	0.53	0.92	6.9
0.05	8.5	25	0.59	1.02	4.0
0.00025	9.6	25	0.41	0.71	305.6
0.001	9.6	25	0.49	0.85	79.1
0.01	9.6	25	0.35	0.62	9.9
0.05	9.6	25	0.45	0.80	0.80
0.01	10.0	25	0.38	0.75	15.1

IV. FRAGMENTATION AND RESTRUCTURING

Our measurement of $D = 2.05 \pm 0.06$ is in agreement with previous measurements of the fractal dimension for slow aggregates, including the original measurements on silica.[5] However, our measurements of the fractal dimension of rapid aggregates show some new features. Previous measurements[6] on unbuffered silica solutions indicate that only two values of the fractal dimension are observed, $D = 1.75 \pm 0.05$ or $D = 2.08 \pm 0.05$, and that sometimes aggregates that initially have a fractal dimension of 1.75 can spontaneously restructure to a fractal dimension of 2.08. For example, aggregates grown at pH 8.5 and a concentration of 0.001 wt % are reported to restructure[6] to a fractal dimension of 2.08 in less than 5 min. Our measurements in buffered solutions at the same pH, shown in Fig. 14, vouchsafe not a clue of restructuring on any time scale. Thus it seems worthwhile to investigate the structural properties of silica aggregates in more detail.

Although restructuring times of hours have been reported in the literature,[6] on these time scales the aggregates sediment to the bottom and must be resuspended by agitation in order to make scattering measurements. The very act of shaking can induce structural changes in the aggregates and it is difficult to determine whether the structural changes thus observed are spontaneous or shear induced. In the following we discuss various mechanical aspects of rapid aggregates, including their susceptibility to shear, pH, and salt concentration.

A. Restructuring experiments

Spontaneous restructuring of rapid aggregates to a higher fractal dimension does indeed seem a reasonable expectation, since it would be surprising for diffusion-

limited growth to generate an equilibrium ensemble. Also, under rapid aggregation conditions there is little time for ripening so that siloxane bonds form between colloidal particles. However, when we attempted to investigate spontaneous restructuring we were impeded by the effects of sedimentation. In the following we describe some of these experiments.

When a concentration of 10^{-3} wt. % silica was allowed to aggregate in a scattering cell at pH 8.5 the scattering data, shown in Fig. 14, show a stable fractal dimension of 1.85 at times from 10 to 120 min. Since spontaneous restructuring was not observed on this time scale, the sample was then gently swirled in the scattering cell; this increased the fractal dimension to 1.94. Shaking the sample then increased the measured fractal dimension to 2.12 as shown in Fig. 16. The shaking may cause internal aggregation of the cluster, with branches attaching to neighboring branches to form compact clusters with circuits. In particular, at small q the scattering data of the shaken sample often have a steeper slope, consistent with a greater collapse on larger length scales, where the clusters are more flexible. Other attempts to measure spontaneous restructuring met with similar results—restructuring was only induced by shear.

To further investigate the possibility of restructuring, 10^{-2} wt. % silica aggregates were grown at pH 9.6 for a total of 17 h. These clusters attain a radius of 1000 nm in only 10 min. Although we hoped that such a long anneal time might encourage structural changes, after 17 hours the aggregates had formed a fine sediment on the bottom

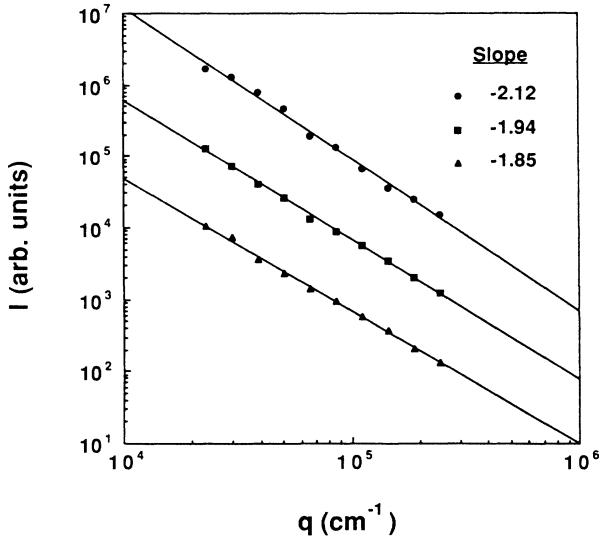

FIG. 16. The effect of agitation on the scattering behavior of aggregates is shown for silica clusters grown at pH 8.5 and a concentration of 10^{-3}%. If this system is unperturbed the scattering is as shown in Fig. 14, with a stable fractal dimension of 1.85. When the sample is swirled, restructuring to a dimension of 1.94 occurs, and when the sample is shaken, the fractal dimension increases to 2.12. These results are not surprising, and simply indicate that the clusters internally aggregate under conditions of shear. The increase in the fractal dimension with internal cluster aggregation has been demonstrated in computer simulations of Meakin (Ref. 14).

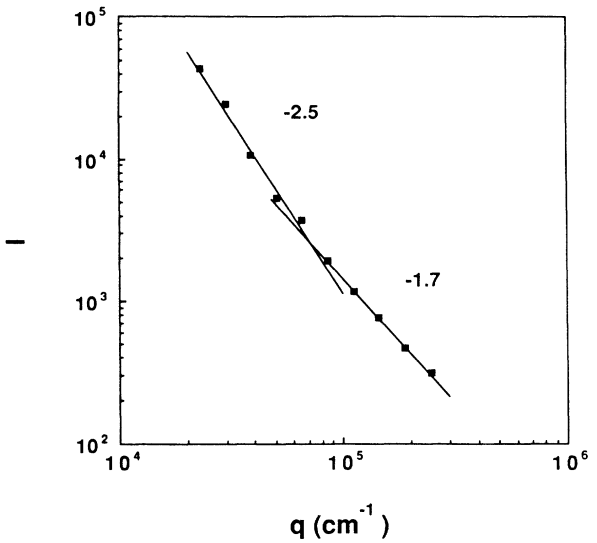

FIG. 17. When aggregates are resuspended, larger structural changes occur. Silica aggregates at $c = 10^{-2}$% were grown at pH 9.6 until sedimentation was complete and the aggregates formed a fine precipitate on the bottom of the scattering cell. After the solution was resuspended the scattering data are non-power-law, with positive curvature on logarithmic axes. Since the low-q slope is greater, one can conclude that greater structural changes occur on larger length scales.

of the scattering cell. This sediment was resuspended by agitation to give an aggregate radius of 1700 nm and the scattering data then taken are shown in Fig. 17. These data are very non-power-law, but do indicate greater collapse on larger length scales. The long anneal time did seem to encourage ripening and made the aggregates somewhat less resistant to the effects of shear.

We were able to produce shear-induced structural changes in other samples as well. For example, samples prepared at 10^{-2} wt. % silica at pH 9.6 gave a dimension of 1.8 after 5 min. Shaking the sample vigorously reduced the cluster radius by half and increased the measured dimension to 2.01. Great sensitivity to shear was observed in samples prepared under very rapid conditions.

When these studies were made at much lower silica concentrations $c = 10^{-3}$ wt. % the aggregates were found to be more stable to handling, but vigorous agitation could still increase the scattering exponent to as much as 2.2. Presumably this is due to the fact that the aggregates have more time to ripen.

In short, we were unable to observe *spontaneous* restructuring to a higher fractal dimension, but noted great sensitivity of the aggregate size and dimension to shear. Similar observations have been made on gold aggregates.

B. Effect of ionic environment

The delicate nature of rapid aggregates is further illuminated in dilution studies. For example, a sample was prepared at pH 8.5 and $c = 5 \times 10^{-2}$ wt. %, allowed to completely settle overnight to allow a maximum time to ripen, and was resuspended by agitation, at which point

the cluster radius was 1300 nm. The sample was then diluted 10:1 into buffer *without* salt and a radius 600 nm was found. A further 5:1 dilution gave a radius of 400 nm and a scattering exponent of 2.2. This decrease in the cluster size with dilution surprised us since it indicated that rapid aggregation in silica might occur in a shallow secondary potential minimum.

The effect of dilution is much more dramatic when the aggregates are not allowed to ripen, as illustrated in the following. At pH 8.5 and $c = 5 \times 10^{-2}$ wt. % growth was allowed for 17 min, giving a cluster size of 2100 nm. A 10:1 dilution into buffer with no salt then gave very small clusters of a radius of 70 nm. After 5 min the radius decreased to 30 nm. Thus it seems that rapid aggregation does indeed occur in a shallow secondary minimum that is highly salt dependent, since increasing the screening length induced spontaneous fragmentation. This effect cannot be attributed to shear alone: an identical sample was aggregated to 2100 nm in 17 min and was then shaken vigorously. This resulted in a decrease to 700 nm—over ten times as large as the diluted clusters.

To further demonstrate that these fragmentation effects are due to the change in charge screening, we repeated the previous experiments by diluting into buffer *with* salt. If the fragmentation under these conditions is smaller, this would show that shear alone cannot explain the dramatic effects we observed. The 10:1 dilution gave relatively large clusters of radius 900 nm (versus 70 nm) with a scattering exponent of 2.2. A futher 5:1 dilution gave 700-nm clusters and a scattering exponent of 2.2. Under these conditions the clusters then continued to grow, indicating that although some shear effect is observed, shear alone cannot account for the size reductions obtained by dilution into a low-salt environment.

A more extensive study of ionic fragmentation was conducted on a sample prepared at pH 8.5 and $c = 10^{-3}$ wt. % (under these conditions 700-nm clusters are produced in 1 h). A 10:1 low-shear dilution by pouring into buffer without salt then gave 250-nm clusters, whereas a high-shear dilution by pipeting gave 110-nm clusters. Thus there is some contribution to the size reduction from the shear fields produced by handling. However, in either case spontaneous fragmentation continued to occur in this low-salt environment; the poured sample decreased to 120 nm after 48 h and the pipeted sample decreased to 90 nm. In contrast, a 10:1 pipeting dilution into buffer with salt gave 540-nm clusters that then aggregated to 2000 nm after 48 h, as shown in Fig. 18, demonstrating conclusively that the fragmentation is due to an increase in the screening length and a change in the shape of the interaction potential.

C. pH and specific salt effects

The solution pH is a strong determinant in the aggregation kinetics, sometimes with surprising results. For example, reducing the pH to 6.7 gives very slow aggregation at higher concentrations, but rapid aggregation at low concentrations. In fact, after 71 h, 22-nm clusters are produced at $c = 5 \times 10^{-2}$ wt. % and 46-nm clusters are produced at $c = 10^{-2}$ wt. %. Likewise, when CsCl salt is used instead of NaCl a dramatic decrease in aggregation rate is observed at high pH, as shown in Fig. 19. For example, at $c = 10^{-2}$ wt. % we studied growth at pH 8.5, 9.6, and 10. At pH 8.5 a radus of 1270 nm was produced after 2.8 min and a dimension of 1.84 was mea-

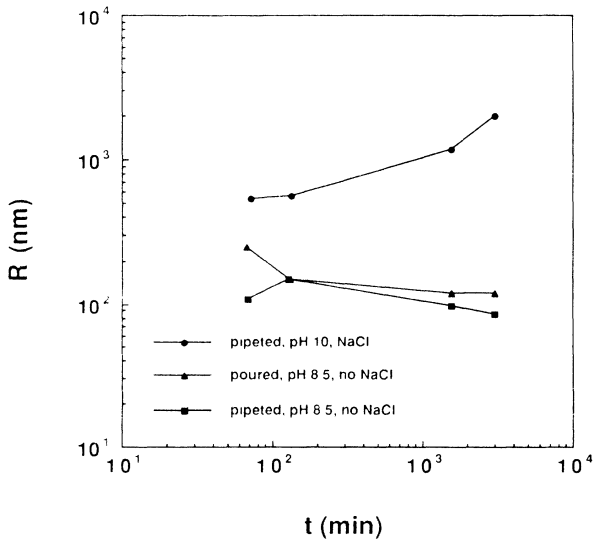

FIG. 18. When rapid aggregates grown at pH 8.5 and $c = 10^{-3}$% are diluted 10:1 into buffer without salt substantial fragmentation occurs, indicating that the interactions that hold the colloidal particles together are reversible. When the dilution is made into rapid growth conditions, at pH 10, cluster formation continues. By contrast, silica aggregates grown under slow growth conditions do not appear to be reversible, probably due to the formation of covalent siloxane bridges (ripening) between particles.

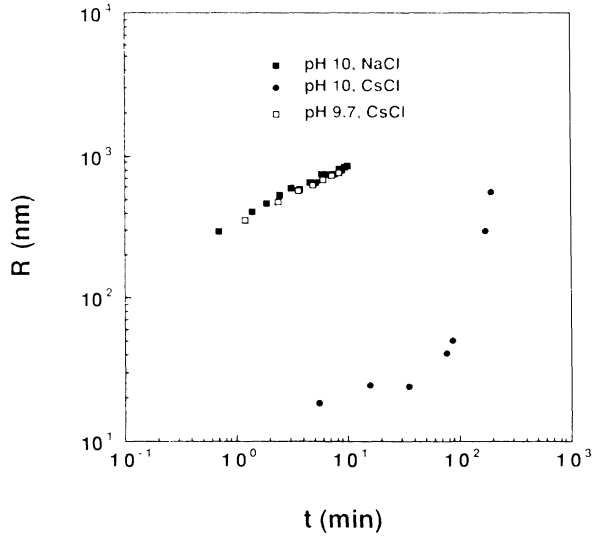

FIG. 19. Growth studies of silica aggregation at $c = 10^{-2}$ % with 1*M* CsCl show a dramatic change in the aggregation rate at pH 10, with a crossover from rapid, power-law aggregation at pH 9.7 to slow, exponential growth (*note*: with 1*M* NaCl aggregation is rapid at pH 10). This change in growth kinetics is accompanied by a change in the fractal dimension from 1.98 under rapid conditions to 2.3 under slow conditions.

sured. At pH 9.6 a radius of 420 nm was produced after 4 min and a slightly larger dimension of 1.94 was determined. Measurements at 25 and 36 min gave clusters of 866 and 950 nm, respectively, and dimensions of 1.94 ± 0.02. Finally, at pH 10 the growth changed from power law to exponential, and after 5 min clusters of a radius of 18 nm were produced. After 190 min these clusters grew to 557 nm and a fractal dimension of 2.3 was observed. When the pH was just slightly less than 10 the aggregation was very rapid, with 566-nm clusters formed in only 3.4 min and an observed fractal dimension of 1.98. Thus a very abrupt transition in the aggregation kinetics and the fractal dimension was observed near pH 10, indicating that the dimension is indeed coupled to the mechanism of growth. However, the relatively large values observed for the fractal dimension indicate that the universality in the aggregation dimension is not that great. With NaCl this transition was not observed; at pH 10 the growth was rapid (590-cm clusters in 3.4 min) and the fractal dimension was 1.83. The nature of this specific salt effect is not understood, but clearly it cannot be rationalized in terms of a screened Coulomb potential.

In another experiment we grew rapid aggregates of low fractal dimension 1.8, reduced the size of these aggregates by a pH quench, and let growth again occur in a slow growth regime to produce aggregates of higher dimension. We prepared a 10^{-3} wt. % solution at pH 8.5, let the clusters grow for 70 min to give a radius of 670 nm, and then quenched the pH to 6.3. This immediately reduced the radius to 100 nm, but after 5.8 h the radius had slowly increased to 400 nm and a dimension of 2.01 was obtained from light scattering. After 7h the radius increased to 446 nm and $D=2.05$ was found, and after 23 hours a radius of 780 nm was obtained and a dimension of 2.05 was found. Thus the rapidly grown aggregates had regrown to a higher dimension under slow growth conditions.

V. CONCLUSIONS

The current description of aggregation is in terms of two universality classes: slow aggregation with exponential growth and $D=2.05$, and rapid aggregation with power-law growth and $D=1.73$. We find that although this is indeed a useful first-order description of the aggregation of silica, there are certain observations that indicate that silica is more complex. For example, fractal dimensions of 1.6–2.0 were found for rapid aggregation under various conditions of concentration, salt, and pH, and fractal dimensions from 2.05 to 2.3 were found for slow aggregation. Also, although power-law growth was observed with a growth exponent $z\sim1$ at pH 8.5, significantly smaller exponents were found at higher pH. Thus the relation $R_z\sim t^{1/D}$ between the fractal dimension and the kinetics of growth is not generally true, although it was observed for 2.5×10^{-4} wt. % silica at pH 8.5. Similar conclusions have been reached for gold,[15] where again the observed growth exponent z was smaller than expected.

The concentration dependence of the growth was also weaker than expected from the constant kernel approximation, especially at pH 8.5, and we were able to demonstrate that in the context of the Smoluchowski equation either a concentration-dependent kernel or a fragmentation term would have to be added to describe these data.

We found that silica aggregates grown under rapid conditions are delicate, showing substantial fragmentation effects with shear and changing solution conditions. Diluting clusters into a low-salt environment demonstrated that the interaction between clusters is easily reversible, unlike slow aggregates, which are robust due to the gradual formation of covalent bonds between particles. Spontaneous restructuring was not observed in any of our experiments, but restructuring was easily induced by agitating the sample. Many of the reported restructuring times are sufficiently long for the clusters to completely precipitate, thus resuspension must have been necessary to make scattering measurements on the clusters. Therefore we believe that the resuspension may be the source of the reported restructuring measurements.

Finally, at pH 10 we observe a dramatic difference between aggregation rates with NaCl and CsCl. This difference demonstrates that the nature of the interaction between these hydrophillic colloids is very complex[18] and cannot be understood in terms of simple charge screening concepts.

ACKNOWLEDGMENTS

This work was supported by the U.S. Department of Energy under Contract No. DE-AC-04-76DP00789.

[1]J. E. Martin and J. P. Wilcoxon, Phys. Rev. A **39**, 252 (1989).
[2]J. E. Martin and K. D. Keefer, Phys. Rev. A **34**, 4988 (1986).
[3]J. E. Martin, J. P. Wilcoxon, and D. Adolf, Phys. Rev. A **36**, 1803 (1987).
[4]J. E. Martin, Phys. Rev. A **36**, 3415 (1987).
[5]D. Schaefer, J. E. Martin, D. Cannell, and P. Wiltzius, Phys. Rev. Lett. **52**, 2371 (1984).
[6]C. Aubert and D. Cannell, Phys. Rev. Lett. **56**, 738 (1986).
[7]J. E. Martin, in *Time-Dependent Effects in Disordered Materials*, edited by R. Pynn and T. Riste (Plenum, London, 1987), p. 425.
[8]M. von Smoluchowski, Z. Phys. Chem. **92**, 129 (1917); Phys. Z. **17**, 585 (1916).
[9]P. G. van Dongen and M. H. Ernst, Phys. Rev. Lett. **54**, 1396 (1985).
[10]B. J. Berne and R. Pecora, *Dynamic Light Scattering* (Wiley, New York, 1976).
[11]J. E. Martin and B. J. Ackerson, Phys. Rev. A **31**, 1180 (1985).
[12]J. E. Martin and F. Leyvraz, Phys. Rev. A **34**, 2346 (1986).
[13]J. E. Martin and D. Schaefer, Phys. Rev. Lett. **53**, 2457 (1984).
[14]For an excellent review of the simulation of aggregation, see P. Meakin, *Phase Transitions* (Academic, New York, 1988), Vol. 12, p. 335.
[15]S. R. Forrest and T. A. Witten, J. Phys. A **12**, L109 (1979).
[16]D. A. Weitz and M. Oliveira, Phys. Rev. Lett. **52**, 1433 (1984).
[17]J. P. Wilcoxon, J. E. Martin, and D. Schaefer, Phys. Rev. A **39**, 2675 (1989).
[18]R. K. Iler, *The Chemistry of Silica* (Wiley, New York, 1979).